The Physical Mechanism of CISK and the Free-Ride Balance

KLAUS FRAEDRICH

Institut für Meteorologie, Freie Universität Berlin, Berlin, FRG

JOHN L. MCBRIDE

Bureau of Meteorology Research Centre, Melbourne, Australia

(Manuscript received 8 September 1988, in final form 30 March 1989)

ABSTRACT

The properties of the "free-ride" assumption of balance between diabatic heating and adiabatic cooling are investigated by incorporating it into the classical two-level CISK (Conditional Instability of the Second Kind) model of Charney and Eliassen. The free-ride model is found to give a CISK-type instability when the heating amplitude exceeds the modified static stability ($S - a\xi$). The free-ride solution is very similar in structure to the CISK solution, except that the free-ride growth rate is independent of scale.

Inspection of the classical CISK model reveals that its growth rate is also independent of scale over the range of scales for which the instability is efficient, and over this range of scales the free-ride and the classical models are essentially identical.

This leads to a new physical interpretation of CISK. Given that the cumulonimbus heating rate is proportional (through the Ekman pumping effect) to the low-level vorticity, the CISK mechanism is interpreted in terms of a balance and a feedback. The balance is the free-ride balance between the (Ekman) heating and the adiabatic cooling by the divergent circulation. The feedback is through increase of the vorticity by the inward advection of angular momentum by the divergent circulation.

This interpretation gives insight into the nature of the CISK mechanism. It explains why the characteristic CISK time scale is half the Ekman spin-down time, and why the space scale is an order of magnitude below the deformation radius. It also reveals that the CISK feedback is through the spinup brought about by the divergent circulation above the boundary layer.

1. Introduction: the free-ride hypothesis of cumulonimbus convection

It has been long known that in tropical weather systems the diabatic latent heat source is an order of magnitude larger than the response in terms of localized rate of temperature change. This has been shown observationally for convection in GATE by Frank (1980) and in radiosonde composite studies of developing tropical cyclones by McBride (1981). It has also been demonstrated by Holton (1972) and Webster (1983) to be consistent with a scaling analysis of synoptic scale variations at low latitudes.

Thus to first order the thermodynamic equation consists of a balance between the diabatic heating and the adiabatic cooling. One of us (JMcB) has been experimenting with the use of this balance as an hypothesis for cumulus parameterization. Assumption of the balance implies that at grid points diagnosed as having convection, the vertically integrated potential temperature tendency can be set to zero. From this context of obtaining a parameterization for free, the assumption of the balance between diabatic heating and adiabatic cooling is referred to here as the "free-ride" assumption. It has been used in numerical models: by Chang (1973) in a simulation of the ITCZ; and by Fingerhut (1978) in a simulation of a steady state cloud cluster. It forms the basis of McBride and Gray's (1980) conceptual theory for the diurnal variation of oceanic tropical convection. Sardeshmukh and Hoskins (1988) adopted it to justify the use of the barotropic vorticity equation to study the generation of teleconnection patterns.

With the above exceptions, however, the free-ride assumption has not been used in tropical dynamics. The aim of the current paper is to begin to explore its theoretical implications. This is done by incorporating it into a well-known simple model of tropical convection, the two-level CISK (Conditional Instability of the Second Kind) model of Charney and Eliassen (1964).

It will be shown that the free-ride version of the CISK model yields a solution almost identical in structure to that of the original CISK model. Also the free-ride growth rate is identical to that of CISK in the range of length scales where the latter shows no scale depen-

Corresponding author address: Klaus Fraedrich, Institut für Meteorologie, Freie Universität Berlin, Dietrich-Schafer-Weg 6-8, D 1000 Berlin 41, Federal Republic of Germany.

dence. This result is surprising as it has been thought (for example, see Emanuel 1986) that the CISK instability inherently depended on a large reservoir of Convective Available Potential Energy (CAPE) such that the diabatic heating was much larger than the adiabatic cooling.

Analysis of the time and space scales characteristic of the original CISK solution reveals that the free-ride balance is not only compatible with CISK but that it also plays a fundamental role in the mechanism of CISK.

CISK has previously been interpreted in terms of a balance and a feedback. Given that the heating through Ekman pumping arguments is proportional to the vorticity, the balance is between the vorticity and the Laplacian of the geopotential perturbation. The feedback is through the modification of the geopotential by the heating. This interpretation is incorrect in that this mechanism is not responsible for the CISK instability.

For the mechanism actually operating in simple CISK models, the relevant balance is the free-ride balance between the Ekman-specified heating and the adiabatic cooling by the divergent circulation. The feedback is the modification of the vorticity by the divergent circulation above the boundary layer.

2. A simple model

The concept of CISK was first formulated by Charney and Eliassen (1964) and Ooyama (1964). The model we have chosen to use here is that of Charney and Eliassen (1964). The characteristics and solution of that model are well documented; it has been studied by Ogura (1964), Charney (1973), and Mak (1981) as well. Henceforth this classical model and solution will be referred to as CEM.

The CEM model is a two-layer model in pressure coordinates for inviscid balanced perturbations about a stratified basic state at rest. Following Charney (1973) and Mak (1981), we choose a slab-symmetric model geometry such that $\partial/\partial X = 0$. Thus all information about the divergence is in the V component and all vorticity information is in the U component of wind. The alternative formulation (Charney and Eliassen 1964; Ogura 1964) is in cylindrical geometry with axisymmetry ($\partial/\partial\lambda = 0$). Then all divergence information is in the radial wind component and all vorticity information in the tangential wind component.

Following Mak (1981), the governing equations are:

$$\begin{aligned} u_t &= fv \\ fu &= -\Phi_y \\ \Phi_p &= -RT/p \\ v_Y + \omega_p &= 0 \\ \lambda T_t &= S\omega p/R + Q^*/c_p, \end{aligned} \qquad (2.1)$$

where the second momentum equation has assumed gradient- (or quasi-geostrophic-) balance, and λ is a trace indicator such that under a free ride assumption λ would be set equal to zero. The terms u, v, ω, Φ, and T are the velocity components in the x-, y-, and p-directions, the geopotential height and the temperature; R is the gas constant, S is the static stability, and Q^* is the cumulus heating to be parameterized. The two-layer model geometry used by CEM is shown in Fig. 1. Expressing vertical derivatives in the corresponding finite difference form, we obtain with the conventional Ansatz (e.g., $v = V(y)\exp\sigma t$) for all variables:

$$\begin{aligned} \sigma U_1 &= fV_1 \\ \sigma U_3 &= fV_3 \\ fU_1 &= -\Phi_{1Y} \\ fU_3 &= -\Phi_{3Y} \\ -\lambda\sigma p(\Phi_3 - \Phi_1)/R\Delta P &= SW_2p/R + Q_2/c_p \\ V_{1Y} + W_2/\Delta P &= 0 \\ V_{3Y} + (W_4 - W_2)/\Delta P &= 0. \end{aligned} \qquad (2.2)$$

The system of equations in (2.2) requires two more relations for closure. These are the Ekman pumping relationship for W_4, and the CISK parameterization of heating:

$$W_4 = KU_{3Y}, \quad Q_2 = -c_p p\xi(W_4 + aW_2)/R. \qquad (2.3)$$

As noted by Chang and Williams (1974), the derivation of (2.3) requires that $U_3 = U_4$, but is standard in the CEM model solution procedure. The friction parameter K is determined by Ekman dynamics of the boundary layer which is assumed to exist below level 4 of the model. It is noted that the heating Q_2 is a generalized form of the CEM heating as used by Charney and Eliassen (1964) and Mak (1981). Ogura (1964) and Charney (1973), however, did not include

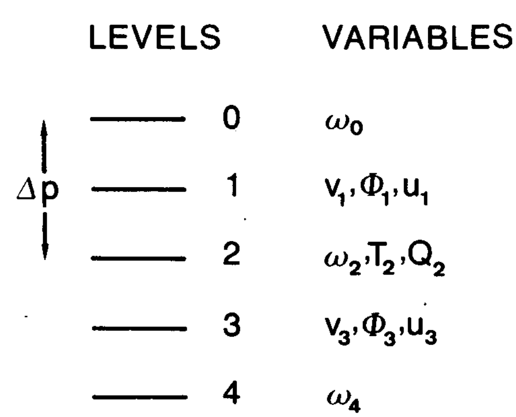

FIG. 1. The two-layer model geometry of the classical CEM CISK model.

W_2 on the right hand side; i.e., they put the coefficient "a" to zero.

By algebraic manipulation, (2.2) and (2.3) can be reduced to the following set of equations:

$$V_1 = -V_3(1 + fK/\Delta P\sigma) \quad (2.4)$$

$$-\Phi_{1Y} = f^2 V_1/\sigma \quad (2.5)$$

$$-\Phi_{3Y} = f^2 V_3/\sigma \quad (2.6)$$

$$W_2 = -V_{1Y}\Delta P \quad (2.7)$$

$$-\lambda\sigma(\Phi_3 - \Phi_1)/\Delta P = (S - \xi a)W_2 - \xi K f V_{3Y}/\sigma, \quad (2.8)$$

where we have used the inner boundary condition that $V_1 = V_3 = 0$ at the origin ($y = 0$) to derive (2.4).

3. The free-ride model

a. Solutions

By its nature the free-ride formulation involves *conditional* heating; thus following Charney (1973) we introduce an inner region ($|y| < b$) characterized by upward vertical motion (i.e., W_2, W_4 negative) and an outer region ($|y| > b$) characterized by sinking motion. The inner region will have cumulus heating, but the nature of the solution will be determined by the free-ride balance, i.e., terms involving the tracer λ will be assumed small. The outer region has no heat, so the heating amplitude ξ is set to zero. For both regions the lower boundary condition is defined by the Ekman relation (2.3). At the lateral boundary ($|y| = b$) they are coupled by the kinematic and dynamic boundary conditions, i.e., by the continuity of mass and pressure.

Differentiating the thermodynamic equation (2.8) with respect to Y and substituting the set (2.4)–(2.7) yields:

$$V_{3YY} - \lambda V_3 \frac{(f/\Delta P)^2(2\sigma + fK/\Delta P)}{(S - \xi a)\left[\sigma + \left(\dfrac{fK}{\Delta P}\right)\left(1 - \dfrac{\xi}{S - \xi a}\right)\right]} = 0. \quad (3.1)$$

The inner region solution can be obtained by putting λ to zero and solving (3.1), subject to the condition that the meridional (i.e., divergent) wind be antisymmetrical about the origin. This procedure yields

$$V_{3i} = -Vy/b, \quad (3.2)$$

where V is a (constant) amplitude of the initial perturbation, and the subscript i denotes a solution for the inner region. By substituting (3.2) into (2.2), inner region solutions can be obtained for all variables.

Alternatively the solution for the inner region can be obtained by putting $\lambda = 0$ in the thermodynamic equation (2.8) and using (2.4), (2.7) to eliminate W_2, yielding $V_{3Yi}[(S - \xi a)(1 + fK/\Delta P\sigma) - \xi fK/\Delta P\sigma] = 0$. For a nontrivial solution, the coefficient in the square brackets equals zero and $V_{3Yi} \neq 0$. This latter condition has a range of solutions of which (3.2) is the simplest.

The solution for the outer region is obtained by putting $\xi = 0$ in (3.1) and solving subject to the antisymmetry of V about the origin. This yields the solution

$$V_3 = -(\text{sign } y)V \exp[-A(|y| - b)], \quad (3.3)$$

where the kinematic boundary condition has been applied at $y = \pm b$, and the lateral e-folding reduction of the CISK signal, A, is defined as the positive root of the relation

$$A^2 = \frac{(f/\Delta P)^2(2\sigma + fK/\Delta P)}{S(\sigma + fK/\Delta P)}. \quad (3.4)$$

Substitution of (3.3) into (2.2) yields solutions for all other variables in the outer region. Matching solutions for Φ at $y = \pm b$, and assuming the geopotential perturbation Φ goes to zero as y approaches infinity provides values for the integration constants in (2.5), (2.6). Thus the complete solutions for the lower model layer are:

Inner region $|y| < b$:

$$V_{3i} = -Vy/b$$

$$U_{3i} = -fVy/\sigma b$$

$$W_{4i} = -KfV/\sigma b$$

$$\Phi_{3i} = \Phi_{30} + f^2Vy^2/2b\sigma$$
$$= -f^2V(b/2 + 1/A)/\sigma + f^2Vy^2/2b\sigma \quad (3.5)$$

and

Outer region $|y| > b$:

$$V_3 = -(\text{sign}\, y)V \exp[-A(|y| - b)]$$

$$U_3 = -(\text{sign}\, y)fV/\sigma \exp[-A(|y| - b)]$$

$$W_4 = KfAV/\sigma \exp[-A(|y| - b)]$$

$$\Phi_3 = -f^2V/\sigma A \exp[-A(|y| - b)]. \quad (3.6)$$

This solution is sketched in Fig. 2. It is noteworthy that the solution in the outer region is identical to the CEM solution given by Charney (1973); for the inner region the upward vertical motion is constant (i.e., independent of y); and the geopotential heights are both continuous and differentiable at the boundary $y = \pm b$.

b. Stability

Setting λ equal to zero in the thermodynamic equation (2.8) and substituting the inner region solution yields an expression for the growth rate:

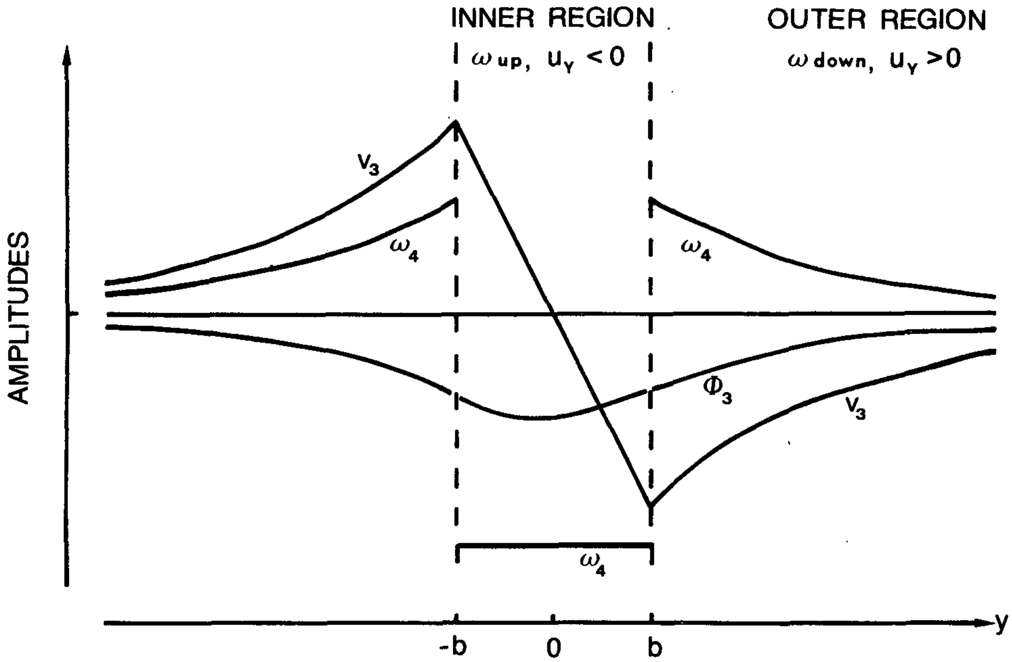

FIG. 2. Sketch of the solutions at the lower layer for the free-ride CISK model.

$$\sigma = \frac{fK}{\Delta P}\left[\frac{(1+a)\xi - S}{S - a\xi}\right]. \tag{3.7}$$

Thus the growth rate is independent of the horizontal scale b, and instability (positive σ) requires that $\xi > S - a\xi > 0$.

c. A posteriori validation of free-ride balance

The underlying assumption of the free-ride balance can be confirmed within the context of this model: that is, T_t is small in comparison with the diabatic heating and adiabatic cooling terms in the thermodynamic equation. We substitute the inner region solution (3.5) into (2.8), set "a" equal to zero and replace ξ by ηS [to allow direct comparison with Charney (1973)]. The condition that the left hand side of (2.8) is smaller than either term on the right hand side then becomes

$$(2 - 1/\eta)^{1/2}b/R + (2 - 1/\eta)(b^2 - y^2)/R^2 < 1. \tag{3.8}$$

The maximum value is at the origin $y = 0$; $R = \Delta P\sqrt{S}/f$ is the Rossby radius of deformation and $A = (2 - 1/\eta)^{1/2}/R$ is the lateral reduction of the CISK signal. With Charney's (1973) numerical value, $\eta = 2.14$, (3.8) reduces to

$$b < R\frac{\sqrt{3} - 1}{(2 - 1/\eta)^{1/2}} \sim 0.6R. \tag{3.9}$$

Noting that b is the half-width of the inner region, this means the free-ride CISK model is confined to scales significantly smaller that 1.2 times the Rossby deformation radius.

4. Comparison with CEM CISK

Equation (3.7) for the growth rate is a familiar one. It is the growth rate for CEM CISK in the small scale limit where the CEM growth rate becomes constant (i.e., independent of scale). This is most easily demonstrated by deriving the CEM growth rate for the case of *unconditional heating.* In that case we can assume a complex exponential form in the y direction, thus replacing y-derivatives by the multiplier il. Setting λ equal to 1, the growth rate is obtained by equating to zero the determinant of the coefficients of the system of Eqs. (2.2) and (2.3). This yields

$$\sigma_{\rm CEM} = \frac{f\Delta PK[(1+a)\xi - S] - f^3K/\Delta Pl^2}{\Delta P^2(S - a\xi) + 2f^2/l^2} \tag{4.1}$$

In the limit as l^2 approaches infinity, it is easily seen that (4.1) reduces to the scale independent free-ride growth rate Eq. (3.7).

Equation (4.1) was studied in detail by Mak (1981) who demonstrated that the terms involving the parameter "a" result over certain length scales in an instability that can be identified with the original conditional instability model studied by Haque (1952), Lilly (1960) and others. Thus to isolate the classical CEM CISK mode we shall follow Ogura (1964) and Charney (1973) by setting "a" equal to zero. Those authors also replaced the heating amplitude ξ by ηS. Following the interpretation of Charney (1973), variations in the numerical value of η are determined by the value of the saturation mixing ratio in the Ekman boundary layer.

Under these conditions, (4.1) becomes

$$\sigma_{\mathrm{CEM}} = \frac{f\Delta PKS(\eta - 1) - f^3K/\Delta Pl^2}{\Delta P^2S + 2f^2/l^2}. \quad (4.2)$$

Defining the length scale $L = \pi/2l$, (4.2) shows that σ is positive for all L smaller than $(\Delta P\sqrt{S}/f)\cdot\sqrt{\eta - 1}\cdot\pi/2$. Also σ_{CEM} is effectively independent of the scale L once the terms involving l^2 in the numerator and denominator of (4.2) are an order of magnitude smaller than the other terms, i.e., once

$$10\cdot L < \min\left(\frac{\Delta P}{f}\frac{\sqrt{S}}{2}\frac{\pi}{2}, \frac{\Delta P}{f}\sqrt{S}\sqrt{\eta - 1}\frac{\pi}{2}\right). \quad (4.3)$$

The numerical value of η is approximately 2.14 (Charney 1973); thus both terms on the right hand side of (4.3) are of the order of the deformation radius $\Delta P\sqrt{S}/f$. Thus the dependence on scale of the CEM growth rate is of the form shown in Fig. 3. The range of scales over which the CEM CISK mechanism is efficient is that range where the growth rate is independent of scale, i.e., the horizontal part of the curve in Fig. 3.

As shown in section 3c, the range of scales for which the free-ride CISK model is self-consistent is that range for which the temperature tendency term on the left hand side of (2.8) is an order of magnitude smaller than the adiabatic cooling SW_2. From (3.9) this is when b is an order of magnitude smaller than the deformation radius. Thus the range of length scales for which the free-ride CISK model is self-consistent is the same range for which the CEM CISK mechanism is efficient.

Therefore, in this range of length scales, *the CEM and the free-ride CISK models are essentially identical.* This is unexpected, as it has previously been thought that the CISK instability resulted from an imbalance between the Ekman-parameterized heating and the adiabatic cooling. Based on the above analysis of the free-ride CISK, in the following section we examine in more detail the balance and feedback mechanisms operating in both CEM and free-ride CISK.

5. The nature of the CISK mechanism

As documented above, the range of length scales over which the classical CISK mechanism is efficient corresponds to the range over which the free ride balance holds. This leads to an interesting insight on the nature of the CISK mechanism.

In simplified form the governing equations for the CISK model can be expressed as follows:

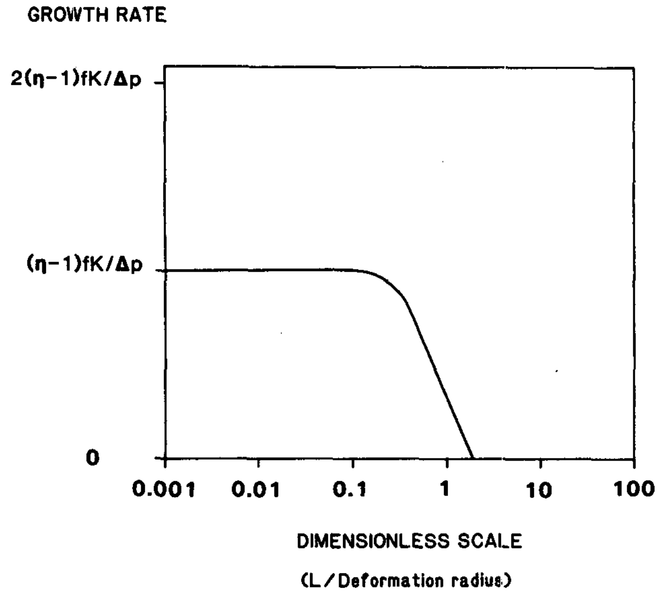

FIG. 3. Variations of the growth rate with length scale for the CEM CISK model.

Balance:

$$\text{Adiabatic cooling} + \text{Ekman heating} = 0$$

$$S(\Delta P\cdot\text{divergence} - K\cdot\text{vorticity}) + \xi K\cdot\text{vorticity} = 0$$

Feedback: (Secondary Circulation)

$$\sigma\cdot\text{vorticity} = -f\cdot\text{divergence}.$$

Substitution of the feedback equation into the balance equation and cancellation of the vorticity as a common term from both sides of the equation yields the familiar CISK growth rate, $\sigma = (fK/\Delta P)\cdot(\xi - S)/S = (fK/\Delta P)\cdot(\eta - 1)$, where it is noted that $2\Delta P/fK$ is the Ekman spin-down time, and at latitude 15° is about 6 days.

Therefore, the physical interpretation of the CISK mechanism is as follows: In regions of cyclonic low level vorticity the upward Ekman pumping of the moist boundary layer air provides the heat source for convective heating of the free atmosphere. On scales significantly smaller than the deformation radius, this heating is identically balanced by adiabatic cooling associated with a divergent secondary circulation. This secondary circulation increases the vorticity through stretching of vortex tubes. The increased vorticity means greater Ekman pumping, hence a greater heat source, which is then balanced by a greater-magnitude divergent circulation. This is a positive feedback loop generating a self-excited disturbance.

The feedback thus works through the vorticity equation $\zeta_t = f\cdot\omega_p$ as is illustrated in Fig. 4. The midlevel condition $\omega_2 = \eta\cdot\omega_4$ is given by the free-ride balance between adiabatic cooling $S\cdot\omega_2$ and CISK heating $-S\cdot\eta\cdot\omega_4$. Also note that substituting $\eta = 1/2$ leads to

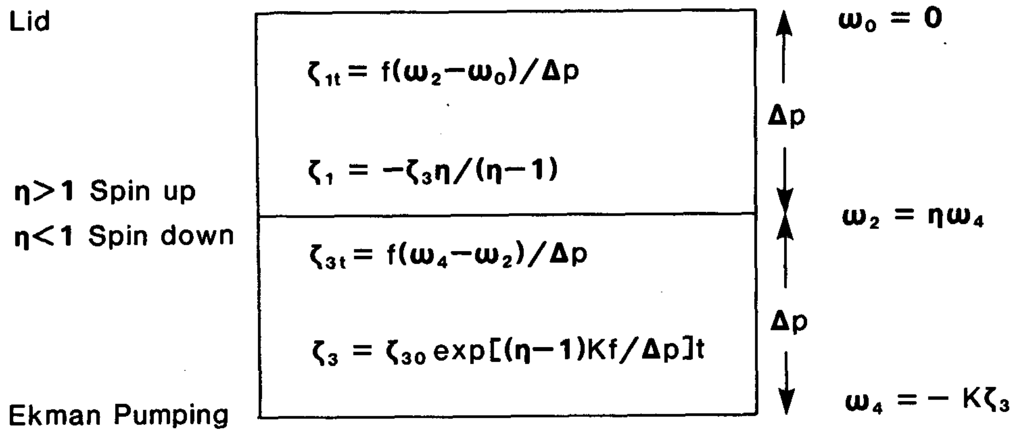

FIG. 4. Vorticity balance of the two-layer free-ride CISK model. Each box includes the vorticity equation for that layer, plus its solution. The upper and lower boundary conditions on ω for each layer are given along the right side of the diagram.

the classical Ekman spin-down problem where $\zeta_1 = \zeta_3 = \zeta_0 \exp - t(fK/2\Delta P)$.

This interpretation explains why the CISK time scale is equal to half the Ekman spin-down time, and why the length scale is approximately an order of magnitude smaller than the deformation radius, the length scale being where the free-ride balance applies. It also shows that the feedback is the spinup associated with the divergent circulation *above the boundary layer.* It also shows that the CISK mechanism is applicable only on space scales such that the width of the disturbance is significantly smaller than the deformation radius.

It is appropriate to contrast this with previous physical interpretations of the CISK mechanism. For example, Charney (1973) states that in regions of cyclonic low level vorticity the upward Ekman pumping of the moist boundary layer air provides the heat source for convective heating of the free atmosphere. He then states, however, that "as heat is liberated in the cyclonic region, the pressure will fall and the geostrophic vorticity will increase, thus leading to a self-excited disturbance." This interpretation assumes the important balance is between the vorticity and the Laplacian of the geopotential perturbation and that the feedback is through the direct response of the pressure to the Ekman heating. This feedback loop cannot, however, be responsible for the instability acting in the classical CEM model since when this feedback equation is substituted into this balance equation, the horizontal scale remains through the Laplacian operator. Thus the growth rate would be inversely proportional to the length scale squared, a property not shown by the CISK model. Also the above balance/feedback combination does not give the Ekman spin-down time as the appropriate time scale; plus it is known from the results of Syono and Yamasaki (1966) and Mak (1981) that the simple CISK instability model is not sensitive to the assumption of gradient balance relationship.

6. Conclusions

We have found that the CISK instability present in the CEM model is dependent on the free-ride balance between diabatic (cumulus) heating and adiabatic cooling. This offers a new interpretation of the physical mechanism of CISK. It can be described by a feedback loop which consists of the following components:

(i) The Ekman pumping relationship induces cumulus heating proportional to the low level vorticity.

(ii) Through the free-ride balance the secondary (divergent) circulation in the free atmosphere is proportional to the cumulus heating.

(iii) The secondary circulation increases the low level vorticity through conservation of angular momentum, which completes the positive feedback loop.

This physical mechanism, dependent on the free-ride balance, explains simply the following features of the CISK instability:

(i) The time scale of the instability is half the Ekman spin-down time.

(ii) The space scale over which the instability is effective is the range an order of magnitude smaller than the Rossby radius of deformation.

(iii) Over this space scale range, the growth rate is independent of space scale.

Acknowledgments. The authors appreciate comments on the manuscript made by Mankin Mak, Kerry Emanuel, Wayne Schubert and two referees.

REFERENCES

Chang, C. P., 1973: A dynamical model of the intertropical convergence zone. *J. Atmos. Sci.*, **30**, 190–212.
——, and R. T. Williams, 1974: On the short-wave cutoff of CISK. *J. Atmos. Sci.*, **31**, 830–833.
Charney, J. G., 1973: Planetary fluid dynamics. Tropical cyclogenesis

and the formation of the intertropical convergence zone. *Dynamical Meteorology,* P. Morel, Ed., Reidel Publ., 331–344.

——, and A. Eliassen, 1964: On the growth of the hurricane depression. *J. Atmos. Sci.,* **21,** 68–75.

Emanuel, K. A., 1986: An air–sea interaction theory for tropical cyclones. Part I: Steady-state maintenance. *J. Atmos. Sci.,* **43,** 585–604.

Fingerhut, W. A., 1978: A numerical model of a diurnally varying tropical cloud cluster disturbance. *Mon. Wea. Rev.,* **106,** 255–264.

Frank, W. M., 1980: Modulations of the net tropospheric temperature during GATE. *J. Atmos. Sci.,* **37,** 1056–1064.

Haque, S. M. A., 1952: The initiation of cyclonic circulation in a vertically unstable stagnant air mass. *Quart. J. Roy. Meteor. Soc.,* **78,** 394–406.

Holton, J. R., 1972: *An Introduction to Dynamic Meteorology.* Academic Press, 319 pp.

Lilly, D. K., 1960: On the theory of disturbances in a conditionally unstable atmosphere. *Mon. Wea. Rev.,* **88,** 1–17.

McBride, J. L., 1981: Observational analysis of tropical cyclone formation. Part III: Budget analysis. *J. Atmos. Sci.,* **38,** 1152–1166.

——, and W. M. Gray, 1980: Mass divergence in tropical weather systems. Part I: Diurnal variation. *Quart. J. Roy. Meteor. Soc.,* **106,** 501–516.

Mak, M., 1981: An inquiry on the nature of CISK, Part I. Tellus, **33,** 531–537.

Ogura, Y., 1964: Frictionally controlled, thermally driven circulations in a circular vortex with application to tropical cyclones. *J. Atmos. Sci.,* **21,** 610–621.

Ooyama, K., 1964: A dynamical model for the study of tropical cyclone development. *Geofis. Int.,* **4,** 187–198.

Sardeshmukh, P. D., and B. J. Hoskins, 1988: The generation of global rotational flow by steady idealized tropical divergence. *J. Atmos. Sci.,* **45,** 1228–1251.

Syono, S., and M. Yamasaki, 1966: Stability of symmetrical motions by latent heat released by cumulonimbus convection under the existence of surface friction. *J. Meteor. Soc. Japan,* **44,** 353–375.

Webster, P. J., 1983: The large scale structure of the tropical atmosphere. *Large-Scale Dynamical Processes in the Atmosphere,* B. Hoskins and R. Pearce, Eds., Academic Press, 235–275.